SANDIA REPORT
SAND2003-8721
Unlimited Release
Printed December 2003

Evaluation of Near-Infrared Tunable Diode Lasers for Detection of Transient Emissions from a Rotary Kiln

C. R. Shaddix, S. W. Allendorf, D. K. Ottesen, P. M. Lemieux, and C. A. Miller

Prepared by
Sandia National Laboratories
Albuquerque, New Mexico 87185 and Livermore, California 94550

Sandia is a multiprogram laboratory operated by Sandia Corporation, a Lockheed Martin Company, for the United States Department of Energy under Contract DE-AC04-94AL85000.

Sandia National Laboratories

Issued by Sandia National Laboratories, operated for the United States Department of Energy by Sandia Corporation.

Available to DOE and DOE contractors from
U.S. Department of Energy
Office of Scientific and Technical Information
P.O. Box 62
Oak Ridge, TN 37831

Telephone: (865)576-8401
Facsimile: (865)576-5728
E-Mail: reports@adonis.osti.gov
Online ordering: http://www.osti.gov/bridge

Available to the public from
U.S. Department of Commerce
National Technical Information Service
5285 Port Royal Rd
Springfield, VA 22161

Telephone: (800)553-6847
Facsimile: (703)605-6900
E-Mail: orders@ntis.fedworld.gov
Online order: http://www.ntis.gov/help/ordermethods.asp?loc=7-4-0#online

SAND2003-8721
Unlimited Release
Printed December 2003

EVALUATION OF NEAR-INFRARED TUNABLE DIODE LASERS FOR DETECTION OF TRANSIENT EMISSIONS FROM A ROTARY KILN

Christopher R. Shaddix, Sarah W. Allendorf, and David K. Ottesen

Combustion Research Facility
Sandia National Laboratories
Livermore, CA 94550

and

Paul M. Lemieux and C. Andy Miller

U.S. Environmental Protection Agency
National Risk Management Research Laboratory
Air Pollution Prevention and Control Division
Research Triangle Park, NC 27711

Abstract

Near-infrared tunable diode lasers (TDLs) were evaluated for their suitability as fast-response combustion performance indicators during tests at the U.S. Environmental Protection Agency's pilot-scale Rotary Kiln Incinerator Simulator (RKIS) facility. Transient emissions (i.e., "puffs") of various magnitudes and duration were generated by injecting a mixture of toluene and methylene chloride into the rotary kiln, through use of a computer-controlled liquid gun or by ram-loading containers of the waste surrogate adsorbed onto corncob. Two wavelength-modulated TDLs that span carbon monoxide (CO) and methane absorption lines at 1.57 and 1.65 μm, respectively, provided information on these species as well as total laser transmittance (an indicator of soot loading). Fiber-optic cables transmitted the laser light from the remotely situated TDLs to two line-of-sight measurement locations. In addition, the TDLs were used with a multi-pass optical cell to perform more sensitive extractive measurements.

Over the optical pathlength available in this facility, *in situ* measurements of methane down to a concentration of ~ 100 ppm were demonstrated during non-sooty conditions. CO could not be reliably quantified *in situ*, even at concentrations as high as 0.7%, due to the combination of weak absorption line strength and interfering water and carbon-dioxide hot-bands. The soot produced during the toluene/methylene chloride puffs typically attenuated over 90% of the TDL laser beam, preventing effective *in situ* TDL measurements during the puffs. In contrast, the extractive TDL measurements demonstrated good accuracy and sensitivity for both methane and CO under all reactor conditions. Furthermore, the *in situ* laser transmittance profiles during the puffs provided new insights into the composition of the puffs as a function of puff magnitude and residence time.

Table of Contents

Page

List of Figures

Page

Acknowledgments

This project was performed with funding from the Environmental Technology Initiative (ETI) program, managed by the U.S. EPA. Ken Hencken and Howard Johnsen of Sandia provided critical technical and logistical support in preparing for and successfully implementing the TDL field test. Gary Hubbard, of Hubbard Associates, programmed the TDL data acquisition, display, and playback software for this project. David Rosenberg, a Sandia co-op student from Cornell University, analyzed the raw TDL signals. The authors would also like to thank A. Touati and Mark Calvi of Acurex Environmental who assisted with RKIS experiment design and operation.

Disclaimer

The research described in this article has been reviewed by the National Risk Management Research Laboratory, U.S. Environmental Protection Agency, and approved for publication. The contents of this article should not be construed to represent Agency policy, nor does mention of trade names or commercial products constitute endorsement or recommendation for use.

Introduction

Rotary kilns are the most common type of incineration system, in part because they are amenable to a wide range of feeding conditions and fuel types (Linak et al., 1987a; Tillman, 1991; Pershing et al., 1993; U.S. EPA, 1993). Currently, rotary kilns and other hazardous waste incineration (HWI) systems are periodically tested to determine the destruction and removal efficiency for specific pollutant emissions: hydrochloric acid, carbon monoxide (CO), particulates, and sometimes total hydrocarbons (THC). However, satisfactory destruction of these species during steady-state testing does not necessarily ensure complete destruction of these or other toxic organic pollutants during short-term transient upset events, or "puffs." Fuel-rich puffs are frequently generated in HWI systems when the hazardous waste feed is introduced in a batch mode, typically as liquid or solid waste in drums or other containers. This type of fuel feeding is particularly common in rotary kilns. When such containerized waste is introduced into an incinerator, the initial fragmentation of the container often results in a rapid release of volatile fuel components, momentarily depleting the local oxygen concentration in the incinerator. Also, for rotary kilns, unsteady exposure of solid or sorbent-bound unburned fuel during the kiln rotation cycle can produce transient, local mixtures depleted of oxygen. These fuel-rich mixtures consequently are convected through the incinerator and can produce significant transient emissions of unburned gaseous hydrocarbons, soot particulate, and CO (Lester et al., 1990; Cundy et al., 1991). The overall emission performance of hazardous waste incinerators is often limited by these transient events. Furthermore, the economics of operating HWI systems that destroy containerized waste is often dominated by the necessity of incurring one to several waste-feed cutoffs each day, due to the formation of large puffs, and permit requirements of maintaining a minimum oxygen (O_2) concentration (typically from 3–5%) in the stack.

Past studies at the EPA's Air Pollution Prevention and Control Division (APPCD) combustion facility have demonstrated that the quantity of unburned gases and particulates produced during a transient upset (i.e., the puff magnitude) in a rotary kiln combustor depends in a complex manner on kiln temperature and rotation speed, waste composition and waste charge size, method of waste injection/packaging, and level of steady and dynamic O_2 enrichment (Linak et al., 1987a, 1987b; Wendt and Linak, 1988; Lemieux et al., 1990, 1992). The magnitude of transient system upsets may be characterized by the amount of O_2 required to completely oxidize the unburned gases and particulates (Lemieux et al., 1995). For typical hazardous waste compositions, the vast majority of the unburned fuel mass in a puff is manifest as hydrocarbons (typically measured on a CH_4-equivalent basis), soot particulate, and CO. Therefore, measurements of these three quantities may be combined to yield a determination of both the instantaneous puff intensity and the time-integrated puff magnitude (Lemieux et al., 1990, 1992, 1995). Furthermore, puffs from different types of fuels or surrogate wastes result in significantly different relative contributions from these three classes of compounds (Linak et al., 1987b; Lemieux et al., 1990). For puffs produced from a given fuel/waste source, one would expect the relative partitioning of unburned mass to shift from hydrocarbon-heavy early in the time-history of a puff to soot-heavy at intermediate times, and then to CO-heavy as oxidation of the puff becomes important.

Transient emissions from incinerators may be minimized by injecting air or pure O_2 into a secondary combustion chamber (SCC), or by modifying the firing rate of the (fuel-lean) afterburner in the SCC. In order to apply one of these control measures, an appropriate sensor in the vicinity of the primary chamber must rapidly indicate the presence of a puff and determine its intensity. As discussed above, the instantaneous puff intensity may be determined by measuring the concentrations of hydrocarbons (or, at least, a surrogate hydrocarbon), soot, and CO.

Unfortunately, conventional continuous emission monitors (CEMs) only exist for hydrocarbons and CO, and practical use of these CEMs necessarily involves a significant gas sampling and conditioning time lag on the order of 30-40 seconds (Lemieux et al., 1995, 1997; Vara-Muñoz et al., 1995). Previous research at EPA's RKIS facility has demonstrated that the slow response of traditional CEMs is a significant hindrance to the development of an effective process control system for the suppression of transient emissions, even when using artificial intelligence (fuzzy logic) to improve feedback control of O_2 addition to the SCC (Lemieux et al., 1995). Typical gas-phase residence times both in the EPA's pilot-scale rotary kiln and in full-scale units are 2 seconds through the kiln section (primary chamber), 2 seconds through the transitional section, and 2–3 seconds through the SCC (Linak et al., 1987a). Therefore, in order to apply effective feed-forward control logic of the afterburner with a detector located at the end of the primary chamber, a detector response time on the order of 1 second (1 Hz) is desired, when accounting for the finite response time of O_2 injection.

In order to achieve a suitably fast response, an optical, preferably *in situ*, sensor is desired for use in incineration systems. As was pointed out by McKinnon et al. (1992), tunable diode laser absorption spectroscopy (TDLAS) is a promising technology for this application, because of its sensitivity to a wide variety of small molecular species, including CO and CH_4, and its ability to accurately measure these species in the presence of complex gas mixtures (as a consequence of the very narrow linewidth of TDLs). Near-IR diode lasers emit extremely narrow (< 0.003 cm^{-1}), single-mode radiation that can be tuned across molecular absorption lines by varying injection current or device temperature near room temperature. This obviates the need for cryogenic temperature-control equipment that is required to operate mid-IR TDLs. In addition, the use of near-IR wavelengths allows the use of inexpensive, commercial-grade fiber optic cabling and fiber splitters to route the output from a single, remote laser source to several detector locations. In contrast to many other laser-based spectroscopies used in the laboratory, near-IR TDL spectroscopy is potentially well suited for application as an on-line industrial sensor, due to its compactness, fast time response, low cost, and the use of reliable and rugged solid-state components (Allendorf et al., 1995, 1997). Unfortunately, the molecular features in the near-infrared are overtone and combination-band transitions, with much weaker absorption line strengths than the transitions in the mid-infrared. Consequently, near-IR TDL sensors are fundamentally less sensitive than mid-IR TDL sensors. Also, in applications with light-attenuating environments (due to soot, ash, dust, or other suspended particulates), the near-IR laser light is usually attenuated more severely than mid-IR light, further reducing the effective sensitivity of the near-IR sensor. The purpose of the measurements described herein was to evaluate the suitability of near-IR TDLs as fast-response puff sensors in incineration systems.

Experimental Setup

Rotary Kiln Test Plan

A series of tests was performed on the EPA's RKIS facility, located in Research Triangle Park, North Carolina. This facility is shown in Figure 1, and is described in detail elsewhere (Linak et al., 1987a,b). Both the main burner and the afterburner are fueled by natural gas and have a firing rate of 250,000 Btu/hr (73 kW). The volumetric heat release rates, gas-phase residence times, and temperature profiles in the RKIS are typical for full-scale rotary kilns, which often have thermal ratings that are 40 times larger. The TDL system was installed on the RKIS facility and made *in situ* measurements at the two port locations indicated in Figure 1, referred to as "burner" and "exhaust" measurements. Fixed-gas CEMs of O_2 (paramagnetic analyzer), CO (NDIR), CO_2 (NDIR), nitric oxide (NO–chemiluminescent), and THC (flame ionization detector–FID) were

sampled at the same nominal locations as the TDLs, using two 1/4-in. (0.635-cm) stainless steel extractive sampling probes inserted perpendicular to the flow. For the transient emission ("puff") experiments, integrated soot loading was measured by collecting soot onto a tared quartz filter maintained in the heated sample line (300 °F, 420 K) used by the THC analyzer.

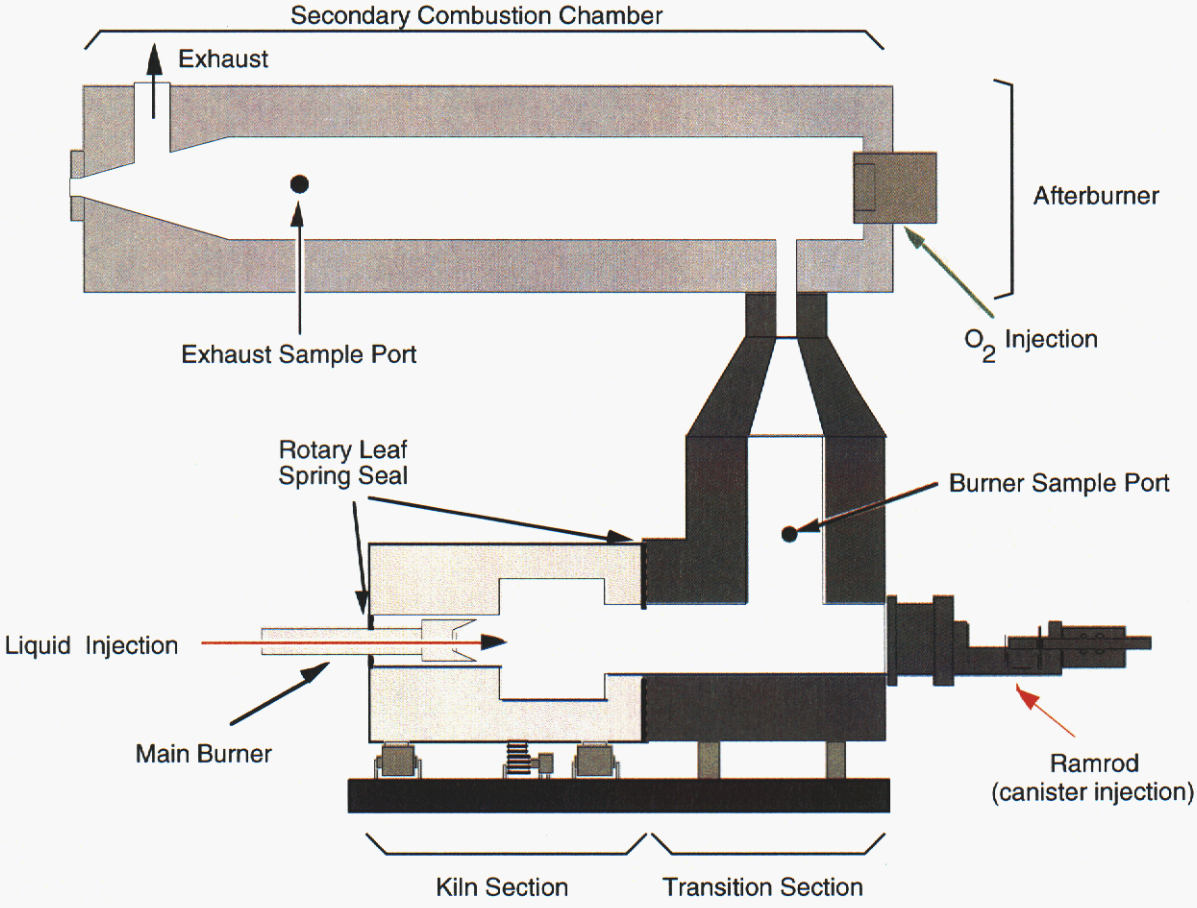

Figure 1. Schematic of the U.S. Environmental Protection Agency's pilot-scale Rotary Kiln Incinerator Simulator (RKIS) facility, showing the locations of liquid and solid injection and the two sampling ports used in this study for line-of-sight TDL measurements across the combustor flow. Stainless steel probes also sampled gases for standard CEM and TDL gas cell measurements at these two locations.

The RKIS tests were conducted in three phases. In Phase 1, the natural gas pilot flames in the kiln section and in the afterburner were run slightly fuel-rich; the stoichiometric ratio [SR = 1/(equivalence ratio)] was 0.85 in the kiln and 0.76 in the afterburner. This test phase allowed a comparison of TDL and extractive probe CEM measurements under quasi-steady, low-sooting conditions. A Tedlar bag sample was analyzed for light HCs to provide a calibration for the *in situ* CH_4 TDL and to compare with the THC CEM.

During Phase 2, the dominant phase of testing, the natural gas burners in the kiln and afterburner were operated slightly fuel-lean (SR = 1.1), and a surrogate liquid waste composed of toluene and methylene chloride (50/50 ratio by volume; 38/62 molar ratio) was injected with a liquid lance into

a region near the RKIS main burner, using a computer-controlled, time-based program. These tests evaluated the time response of the TDL detector system and its ability to detect and quantify system transients (puffs). The time-dependent injection rate of surrogate waste (W) followed the equation:

$$W = PI * | \sin(n\pi t/\tau) | \quad (1)$$

where W is the instantaneous flow rate of surrogate, PI is the maximum surrogate flow rate, n is an integer ranging from 1 to 3 that determines the number of consecutive, identical puffs, t is the time in seconds, and τ is the desired puff duration in seconds (Lemieux et al., 1990). PI values of 0.037-0.046 mol/s and τ values of 100-300 seconds were used during these experiments. Each set of conditions was repeated three times, for 39 total experiments. The experiments were performed in a random matrix, to eliminate biases from the gradual increase of kiln temperature (temperature creep) that normally occurs due to the imposition of many high temperature transients on the incinerator. The injection of surrogate waste and run initiation times were triggered by a digital switch that simultaneously started the integrators on the RKIS data acquisition system and sent a signal to the TDL system so that timescales could be synchronized.

Test Phase 3 consisted of more realistic puff conditions produced by the ramrod injection into the kiln of 1-qt (0.9-L) cardboard containers filled with corncob sorbent. The 50/50 (by volume) toluene/methylene chloride mixture was bound on the corncob, with a total container weight of 200 grams. Two characteristic puff magnitudes were generated, using either 60 or 80 mL of total "waste" dopant in a container. The kiln rotated at 0.45 rpm. Sixteen separate experiments were conducted during this portion of the testing.

TDL Equipment

A single data acquisition system was designed to simultaneously operate two near-IR tunable diode lasers. One TDL scanned across the R(1) line of the 0–>3 overtone band of CO at 6357.8 cm^{-1}, or 1572.9 nm (in vacuum). The other TDL scanned across the R(2) doublet of the $2\nu_3$ band of CH_4 at 6036.7 cm^{-1}, or 1656.5 nm (in vacuum). These diode lasers are near-IR InGaAs/InP (Indium-Gallium-Arsenide/Indium-Phosphide) distributed feedback devices that have been packaged into temperature-controlled modules compatible with the electronics of the Bovar Western (formerly Spectrum Diagnostix) ammonia monitor (SpectraScan™). Custom software has been developed to allow dual modulation of the laser wavelength. The laser is scanned slowly (213 Hz) across ~ 1 nm (0.5 cm^{-1}) with a ramp waveform to selectively detect the molecule of interest. A fast (1 MHz) sinusoidal wavelength modulation over approximately one absorption feature linewidth is superimposed on the slow spectral scan. Phase-sensitive detection at twice the driving frequency (2 MHz) selectively amplifies the molecular absorption feature and results in significantly enhanced sensitivity over direct absorption (Silver, 1992; Cooper and Martinelli, 1992; Allendorf et al., 1994). This second-harmonic detection of the high-frequency modulation results in a spectral feature with a shape similar to the second derivative of the absorption lineshape. In the linear response region, the magnitude of the second-harmonic feature is proportional to the molar concentration of the absorbing species (for a given temperature and pressure) (Cooper and Martinelli, 1992). For optimal molecular sensitivity, both a slow-scan and 1-MHz sinusoidal waveforms may be imposed across the absorption feature linewidth and dual lock-in amplifiers applied, resulting in a dc signal proportional to the local absorption depth. However, this "monitor mode" technique does not provide any information about the local absorption spectrum and is sensitive to transient broadband absorption of the laser beam. Instead, for this application we use the slow spectral scan method, in which only a single lock-in is used to demodulate the high-frequency modulation. With spectral scan detection, the time-dependent behavior of molecular

interferences, optical etalons, and attenuation of the laser beam may be evaluated. For *in situ* applications in which a particulate-laden gas stream may be sampled, the broadband absorption of the laser beam needs to be evaluated, because the magnitude of the molecular absorption feature is proportional to the total amount of laser light incident on the detector. For the modulation depth used here, the CH_4 doublet appears as a single, relatively wide absorption feature.

The pigtailed fiber optic output from each diode was split into three fibers (see Figure 2). One of the fibers transmitted the laser beam to a reference cell, whereas the other fibers transmitted the laser beam to the two sampling locations. The reference cells are small, enclosed Herriott cells with a total pathlength of 10 meters. They were maintained at room temperature and a pressure of ~ 200 torr. The reference cells were used to verify the laser scan wavelength and also were used to actively line-lock the diode lasers on their prescribed absorption features (to prevent laser wavelength drift over time). Small optical breadboards containing the laser sending and receiving optics were attached to nitrogen-purged 3-in. (7.6-cm) American National Standards Institute (ANSI) flanges on the incinerator. GRIN (gradient index of refraction) lenses were used to launch the laser beams from the single-mode optical fibers. In order to increase the sensitivity of the *in*

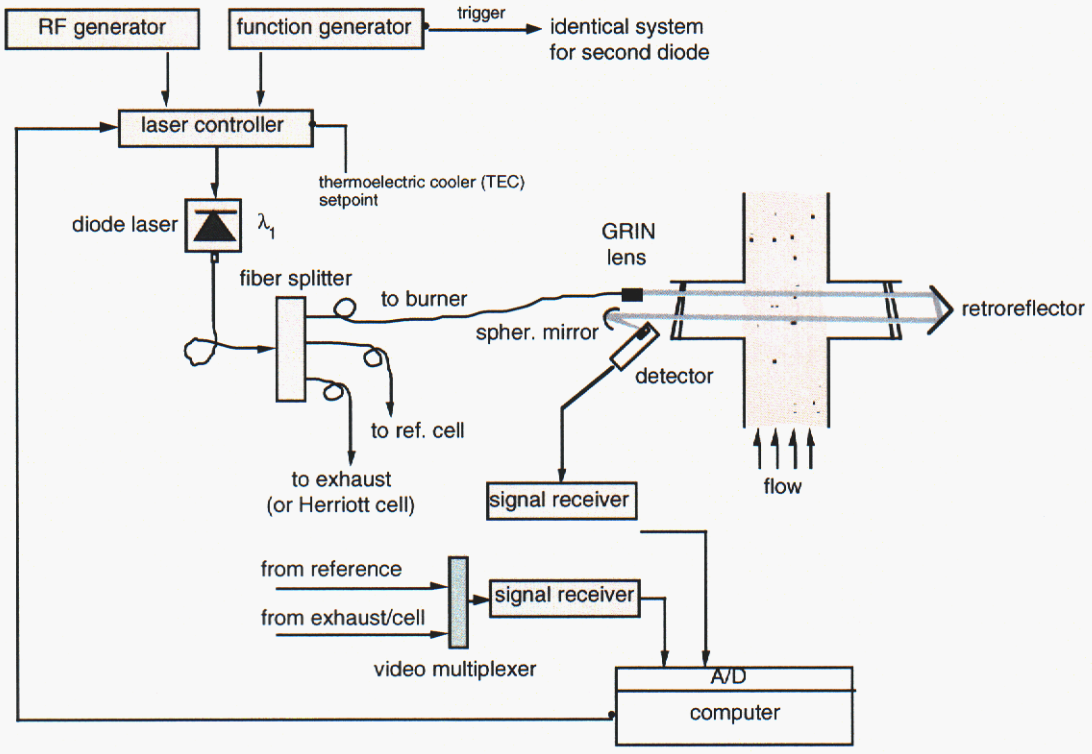

Figure 2. Schematic of the diode laser control, launch, and detection system. As indicated at the top of the figure, the slow ramp function generator for one of the diodes triggered the function generator for a second diode, whose layout is identical to that shown here (i.e., two GRIN lenses, two spherical mirrors, and two detectors were situated on the breadboards at each *in situ* measurement location).

situ measurement, retroreflectors were used to double the effective duct flow sampling width to 36 in. (91 cm) at the burner port and 48 in. (122 cm) at the exhaust port. The total distance traversed from window-to-window across the incinerator was 6 ft. (1.8 m). In order to reduce optical etalon

effects, anti-reflection (AR)-coated, 3°-wedged quartz windows were canted at 15° in the flange connections. Spherical mirrors at near- normal incidence were used to focus the transmitted laser beam onto high-speed InGaAs detectors. Signal receivers demodulated the detector outputs and sent both low-pass filtered raw detector signal (so-called "0f") and the demodulated ("2f") signal to a computer. The computer digitized and stored 100-scan averages of the detector signals for each laser at each measurement location, resulting in net data rates of ~ 1 Hz. The 0f signals were post-processed to determine the time history of the laser transmittance, in order to correct the measured 2f signals for transmittance variation and to calculate the instantaneous soot particulate concentration in the sample volume. Sample demodulated signals from the reference gas cells and the *in situ* measurement are shown in Fig. 3. The greater width of the 2f signal feature for the CH_4 in situ measurement, in comparison to the CH_4 reference gas cell, indicates that the CH_4 absorption feature is broader in the burner environment than in the reduced pressure gas cell.

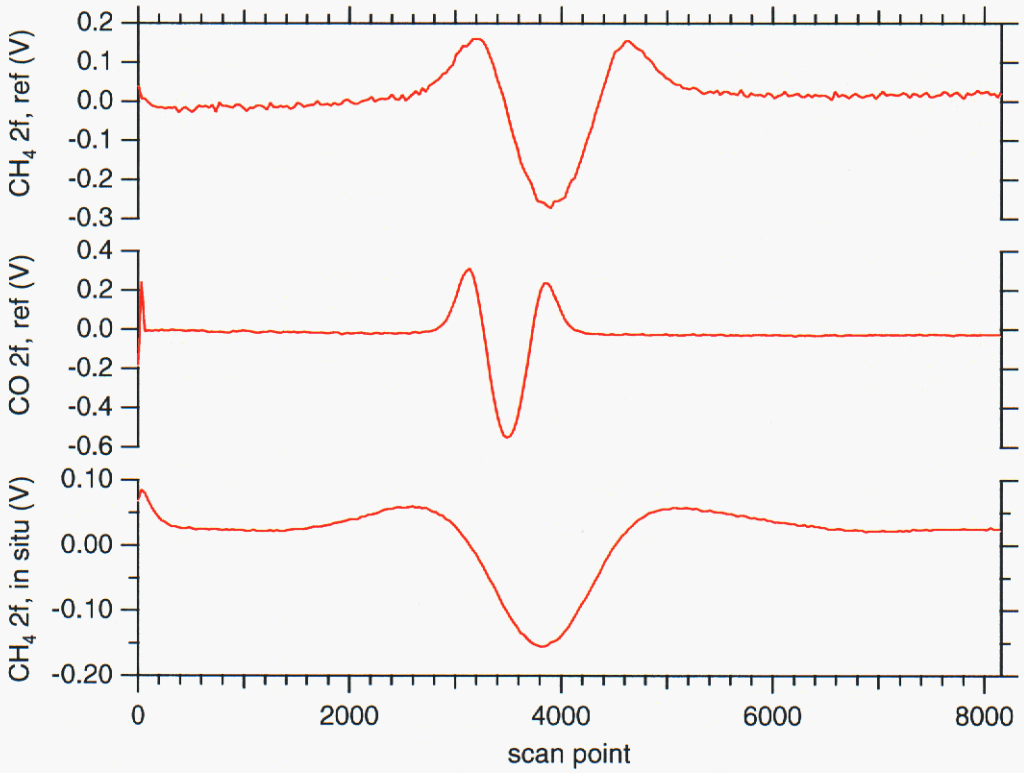

Figure 3. Second-harmonic lock-in signals from the TDL laser scans. All signals are 100-scan averages. The top two scans are from the reference gas cells and the bottom scan is from the *in situ* measurement at the burner sample location during fuel-rich combustion of natural gas.

TDL Gas Cell

The primary goal of the present project was to investigate the applicability of near-IR TDL sensors for *in situ* measurements (due to their inherently fast response). However, TDL measurements were also made by flowing extractive probe-sampled gases through a multipass Herriott gas cell with a 10-m pathlength. These latter measurements provided a more accurate determination of gas species concentrations by TDL for comparison with standard CEMs. These measurements were performed by accessing the CEM sample flow from the burner location, after it had undergone gas conditioning (including removal of water vapor). The gas cell can only accommodate a single fiber optic transceiver, so for each of the latter two test phases the fiber optic for one of the TDLs was relocated from the exhaust sampling position to the gas cell (the CO fiber was relocated during Phase 2 and the CH_4 fiber was moved during Phase 3). Extractive TDL measurements are more sensitive than *in situ* measurements for several reasons. First, the multipass configuration of the optical cell directly increases the absorption pathlength (in this case, to 10 m versus the 0.9 m *in situ* absorption path) and thus the sensitivity. Also, pressures and temperatures can be reduced in an extractive cell (300 torr and near-ambient temperature were used for this project). Detection at lower pressure narrows the collision-broadened linewidths, resulting in stronger on-peak signals. Also, interferences due to other molecular species present in the gas flow are generally reduced because their absorption linewidths are similarly decreased due to a lower pressure in the gas cell. At lower temperatures, fewer high energy states are populated, resulting in a larger population in the lower energy states of the target molecule and a reduced likelihood for spectroscopic interference from hot-band transitions of other molecules (especially CO_2 and water). All of these effects lead to relatively stronger, more easily detected molecular signals in an extractive measurement compared to an *in situ* measurement. Finally, extractive gas measurements have the important feature of direct calibration by flowing a calibrated gas mixture through the cell. Such a direct calibration is generally difficult, if not impossible, for an *in situ* technique. The CO and CH_4 TDL detectors on the extractive gas cell were calibrated each day before performing any tests by passing the appropriate CEM span gases (0.1 and 2% CO, 80 and 800 ppm CH_4) through the cell. The TDL signals exhibited good linearity over these concentration ranges.

Results and Discussion

Steady Combustion Experiments

Figures 4 and 5 compare *in situ* TDL measurements of CO and CH_4 with those from conventional extractive-sampling CEMs during "steady," non-sooty operation of the kiln (Phase 1 testing). Fig. 4 delineates the relative response over an extended period of time (1000 s), whereas Fig. 5 focuses on the relative behavior over a shorter time scale (200 s) within this overall period. It is apparent from these figures that, even under nominally steady combustion conditions, the production of PICs (products of incomplete combustion) can show substantial temporal variations due to turbulent mixing and incinerator exhaust damper cycling. The time records of the TDL signals reveal that the *in situ* laser measurement (with a time response of < 2 seconds) responds ~ 20 seconds faster than the THC CEM and ~ 30 seconds faster than the CO CEM (see Fig. 5). In addition, comparison of the time trace of the CH_4 TDL signals versus that of the THC CEM demonstrates that the CH_4 TDL yields sensitive, quantitative results with *in situ* detection. In contrast, the CO TDL signal suffers from significantly weaker line strengths in the detected spectral region and interference from CO_2 and/or water hot-band absorption lines. Consequently, the *in situ* CO TDL signals do not accurately track the CO measured with the NDIR CEM at the measured

concentrations of 0.4 ± 0.3%. Some consistency in temporal behavior is seen (e.g., the occurrence of the two peaks between times of 500 and 750 seconds in Fig. 4), suggesting that the *in situ* TDL measurement of CO is near its detection limit for these CO concentrations.

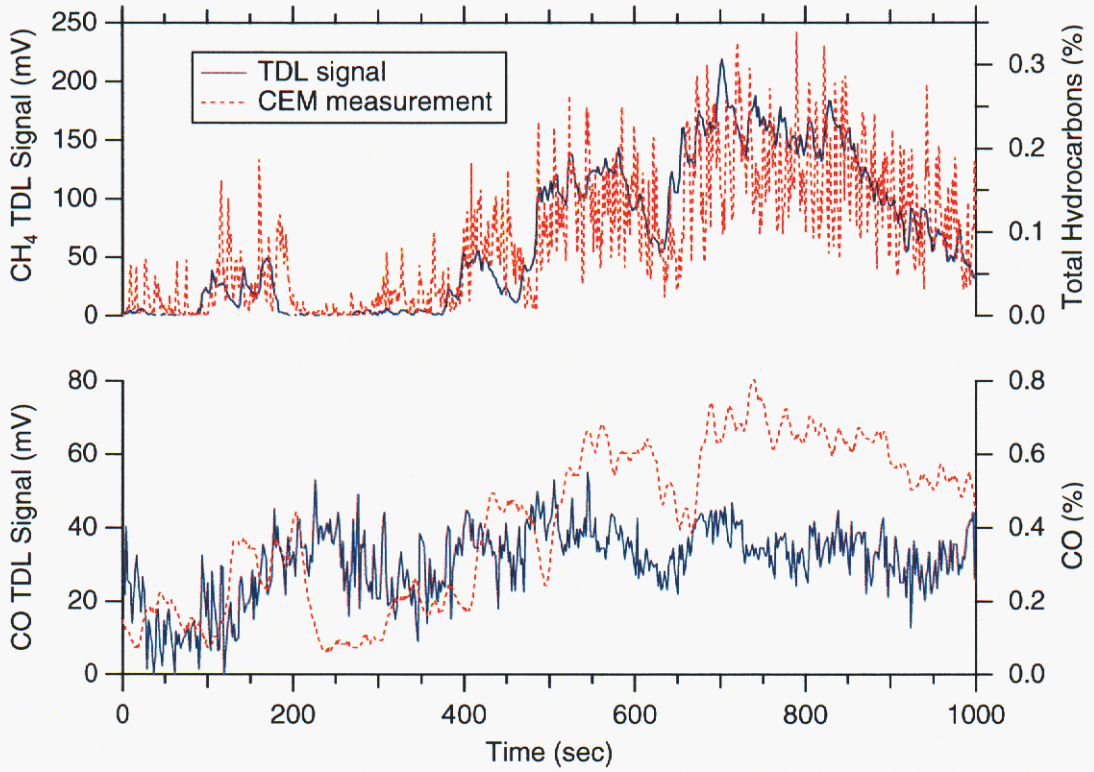

Figure 4. Time record of *in situ* TDL signals and corresponding CEM measurements from the RKIS burner sample location during operation of the kiln pilot flame on natural gas, under slightly fuel-rich conditions (ϕ = 1.2). Note the smaller magnitude of the CO TDL signals in comparison to the CH_4 signals.

A Tedlar bag was used to sample 20 minutes of flow from the exhaust probe position during one of the Phase 1 tests and was analyzed using gas chromatography. Comparison of the 2200 ppm of CH_4 measured from the bag sample with the integrated THC measurement during the same sampling period yields a CH_4/THC ratio of 0.7, which is not unexpectedly high considering that the source of the exhaust gas was a fuel-rich natural gas flame. Using this value in concert with the TDL data in Figs. 4 and 5, it is estimated that the *in situ* detection limit of the CH_4 TDL (at 1930 °F = 1330 K) is 100-200 ppm.

Liquid Injection Puffs

Figure 6 shows typical TDL and CO CEM measurements during a series of puffs generated in the rotary kiln by the time-controlled injection of a mixture of toluene and methylene chloride (Phase 2). Copious quantities of soot were visually observed to be present in the incinerator during these puffs. With the generation of soot in the kiln, strong attenuation of the laser beam occurred inside

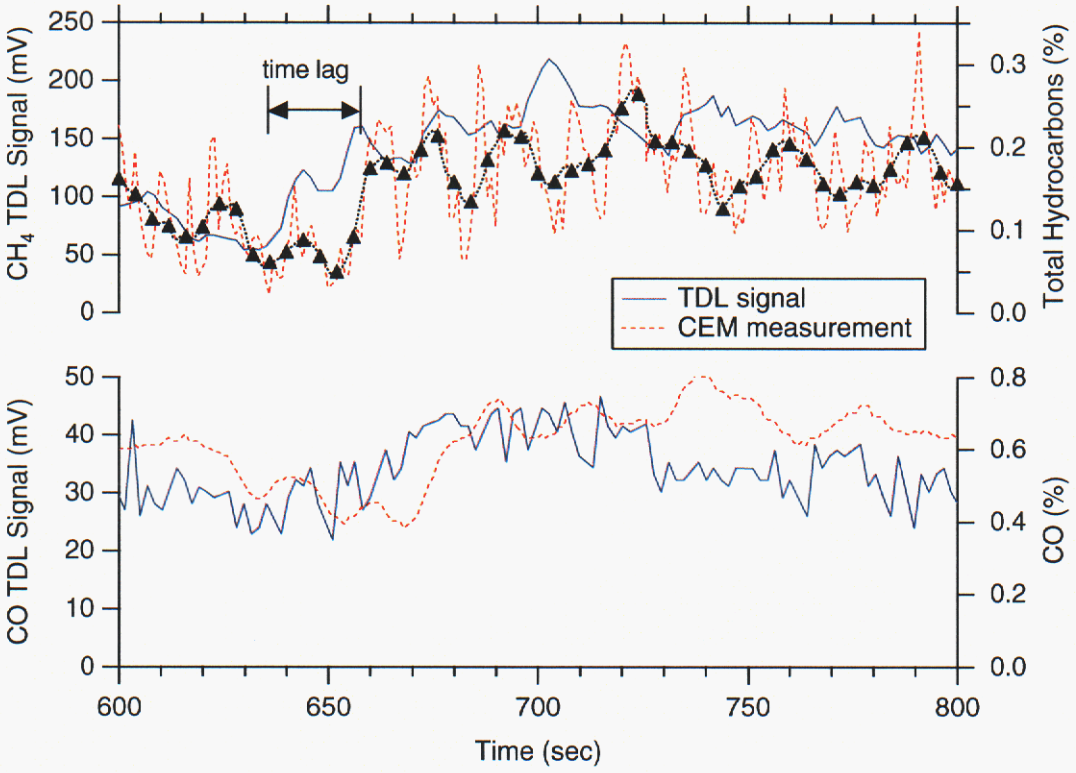

Figure 5. Expanded view of time record shown in Fig. 4. The triangles in the THC CEM trace denote smoothed values of the time record, which assist in evaluating the time delay between the TDL CH_4 signal and the noisy THC CEM output.

the kiln, as indicated in the top half of Fig. 6, and prevented the *in situ* measurement of CO and CH_4 for all of the puffs produced in this test series. However, this loss in transmittance in itself provided a sensitive, rapid puff indicator. In addition, the CO TDL analysis of extractively sampled, filtered gases provided an accurate measure of CO concentrations, as demonstrated in the lower half of Fig. 6. Although the gas sample for the TDL gas cell passes through all of the piping associated with the sample probe and sample conditioning system, the near-instantaneous response of the TDL results in an approximately 10-second faster peak response time for the TDL gas cell measurement in comparison to the CO CEM. The additional time-lag of the CO (and CO_2) CEM results from the use of a typical, long response time setting (for improved readout accuracy) on the NDIR instrument during these tests. The only gas conditioning required for successful operation of the TDL gas cell is particle filtration. Consequently, a dedicated sampling line with the gas cell mounted close to the incinerator should yield an extractively-sampled, highly-sensitive TDL measurement of gas composition within a few seconds.

During both the Phase 2 (liquid-injection puffs) and Phase 3 (canister-generated puffs) experiments, the TDL laser beam was almost completely attenuated during the passage of the puffs across the optical sampling locations. Because of the linear dependence of the molecular concentration (2f) signal strength on the laser transmittance, this attenuation of the TDL beam resulted an insufficient signal-to-noise ratio for successful *in situ* measurement of CO and CH_4

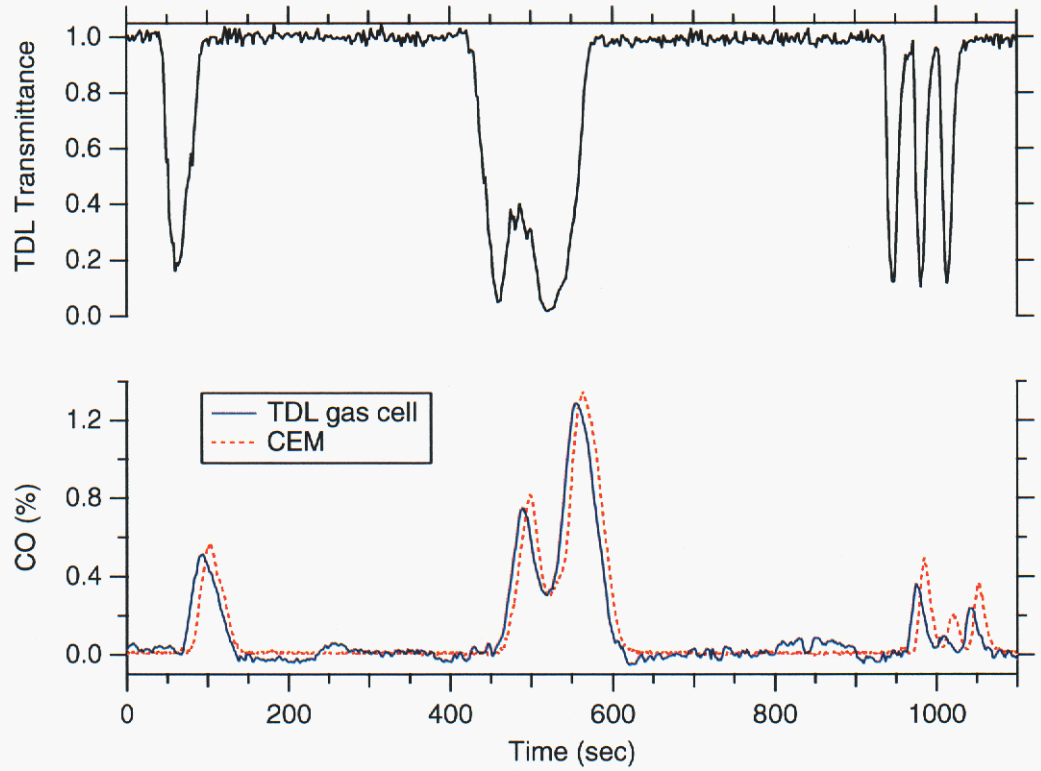

Figure 6. Time record of TDL signals and the CO CEM measurements from the RKIS burner sample location during a series of methylene chloride/toluene puffs generated by computer-controlled injection of the waste surrogate into the kiln. The top plot shows TDL laser transmittance from the in situ measurement and the bottom plot shows results from the extractive measurements.

concentrations during the puffs, despite the elevated concentrations of these gas species within the puffs. Figure 7 displays the CO and hydrocarbon CEM measurements together with TDL-derived soot concentrations (discussed later) at both the burner and exhaust sampling positions for some of the liquid-injection puffs (for a different puffs than those shown in Fig. 6). Figs. 6 & 7 show that peak CO levels in the liquid-injection puffs were around 1.5%, whereas peak total hydrocarbons were about 1000 ppm. With a typical maximum attenuation of ~ 95% of the incident laser beam during the passage of a large puff, the minimum detection limits determined during the steady combustion tests (7000 ppm for CO and 200 ppm for methane) translate to expected minimum detection limits of 14% for CO and 4000 ppm for methane for *in situ* TDL measurements during the peak of the puffs. In fact, peak CO and THC levels in the puffs, as measured by the extractive CEMs, were in the vicinity of 1.5% for CO and 1000 ppm for THC. The *in situ* TDL signals were scrutinized during the rising and falling edges of the TDL transmittance profiles for evidence of CO or CH_4, but no definitive gas absorption features were evident. If TDL data collection had occurred with more limited time-averaging of spectral scans (100-pt. averages were stored during these tests), molecular signals at the rising and falling edges of the puff profiles may have been successfully resolved.

The baseline concentrations of CO and total hydrocarbons as measured by the CEMs between puffs were 15-60 ppm and 0-20 ppm, respectively, which is well below the *in situ* TDL detection

limits. Consequently, the only available *in situ* TDL signal during the liquid-injection (and canister-injection) tests was the laser attenuation. Operation of the kiln with a less sooty waste fuel mix would potentially reduce the laser attenuation during puffs to a level that remains acceptable for performing the *in situ* species measurements. Aromatic compounds (such as the toluene portion of the waste simulant used in these experiments) are known to be exceptionally prone to soot formation in fuel-rich environments (Glassman, 1988). Furthermore, the use of chlorinated hydrocarbons (such as the methylene chloride used here) generally exacerbates the sooting tendency of flames or pyrolytic processes (Morse and Cundy, 1994). Therefore, the surrogate waste combination used in this study probably represents a severe sooting mixture compared to the range of wastes of interest to commercial incinerators.

Derived Soot Concentrations

The measurements of laser attenuation may be used to derive the instantaneous soot concentration in the flow, as long as there is not a significant contribution of ash particles to the transient laser light attenuation. Feeding of fly ash was performed in some of the experiments, but the feed rate was nominally steady and did not appreciably affect the TDL laser transmittance. The instantaneous, optical path-averaged soot concentration, expressed as volume fraction, is derived from the transmittance time record by applying the Bouguer-Lambert law for light absorption in a uniform medium:

$$I/I_0 = \exp\left(-\frac{K_e}{\lambda} f_v l\right) \qquad (2)$$

where I is the transmitted laser intensity, I_0 is the initial laser intensity, K_e is the non-dimensional extinction coefficient, λ is the laser wavelength, f_v is the soot volume fraction, and l is the absorbing pathlength. For particles with a characteristic size that is much smaller than the laser wavelength, the extinction coefficient is equal to the product $6\pi E(m)$, where E is a prescribed function of the complex index of refraction, m (Bohren and Huffman, 1983). This Rayleigh-limit expression for K_e has been widely utilized for interpretation of laser extinction measurements of soot concentration, even with visible wavelength laser sources. However, a wide range of values has been measured for soot indices of refraction, leading to a large uncertainty in the choice of any particular measured value (Smyth and Shaddix, 1996). Also, aggregated soot particles, as expected at the measurement locations in this study, frequently fall outside of the Rayleigh limit and produce non-negligible scattering contributions to the overall laser extinction. A number of measurements have been recently performed on the non-dimensional extinction coefficient of postflame soot formed in laminar and turbulent flames of a wide variety of fuels (Mulholland and Choi, 1998; Krishnan et al., 2000; Zhu et al., 2000; Krishnan et al., 2001; Zhu et al., 2002; Widmann et al., 2003). These measurements have consistently yielded extinction coefficients that are substantially larger than those predicted from Rayleigh theory when using past measurements of the soot refractive index. In particular, at the ~1.6 μm wavelength of the CO and CH_4 lasers used in this study, a K_e of 9–10 was recently reported for soot derived from acetylene and ethylene flames (Zhu et al., 2002). In comparison, Rayleigh-limit extinction coefficients derived from canonical soot refractive index values reported by Dalzell and Sarofim (1969), Lee and Tien (1981), and Habib and Vervisch (1988) are equal to 6.1, 5.1, and 3.3, respectively, using the dispersion relations evaluated at 1.6 μm. For the analysis of the TDL laser attenuation in this study, a K_e of 9.2 is assumed, as is supported by the recent measurements at both 1.3 and 1.6 μm (Zhu et al.,

2002). The estimated uncertainty in using this value of K_e and therefore in the derived soot concentrations is on the order of ± 15%.

Figure 7 compares a typical time trace of TDL-derived soot concentrations at both sampling locations with the corresponding readouts from the THC and CO CEMs. The faster response of the TDL reading is evident, as well as peak soot volume fractions on the order of 0.5–1 x 10^{-6} (i.e., 0.5–1 ppm). At a given sampling location, the peak soot concentration during the passage of puffs roughly scales with the peak CO concentration. However, the proportionality constant varies from the burner sampling location to the exhaust. For an on-line sensor to provide accurate feed-forward logic for operation of the kiln afterburner, an immediate reading such as this of the soot concentration is needed. Past experiments on afterburner process control have neglected the contribution of soot to the total unburned material in a puff, because of the lack of an available "soot CEM" (Lemieux et al., 1995).

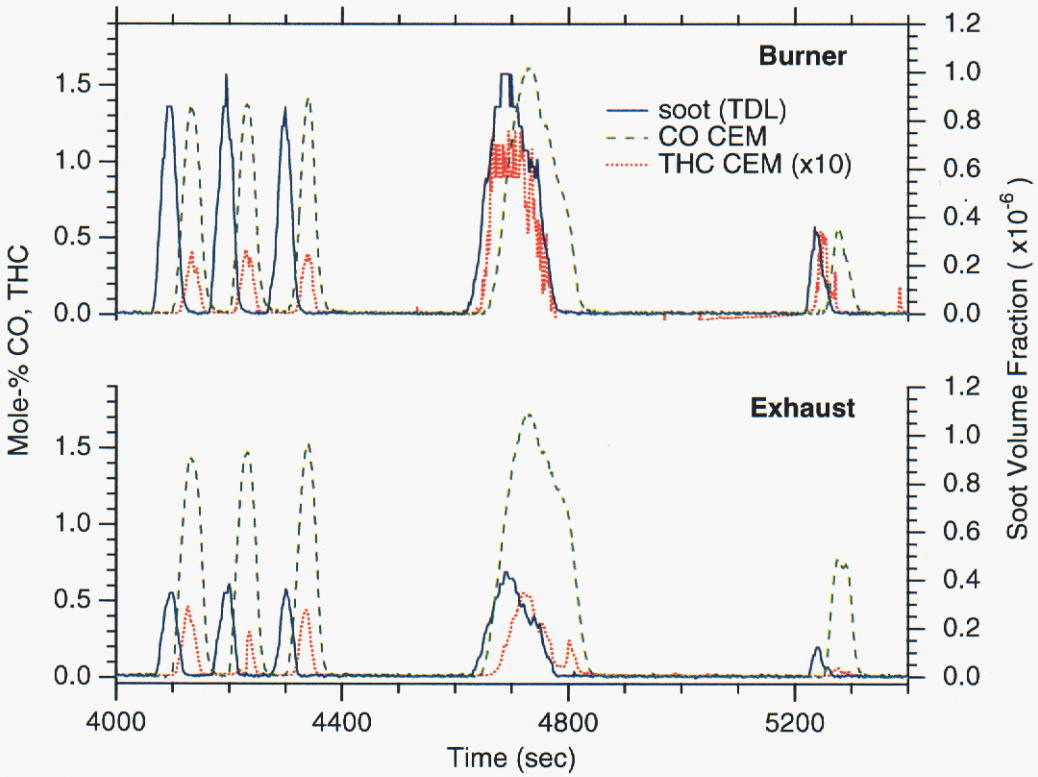

Figure 7. Time record of TDL attenuation-derived soot volume fraction and the CO and total hydrocarbon (THC) CEM measurements from the two RKIS sample locations. Puffs were generated by computer-controlled injection of methylene chloride and toluene into the kiln.

The TDL transmittance-derived soot concentrations may be compared with those determined by extractive sample filter capture over the course of each puff test series, which consisted of one to three discrete puffs. In order to convert the transmittance-derived soot volume fractions to time-integrated soot mass, the local volumetric flow rate and density of soot are required:

$$m_s = \rho_s \dot{V} \int f_v dt \quad . \tag{3}$$

A typical value of 1.9 g/cm^3 is assumed here for the soot density, ρ_s. The local volumetric flowrate, $\dot{V}$, is determined by multiplying the volumetric flowrate at standard conditions by the ratio of the local temperature to the standard temperature (298 K). Thermocouple measurements in the incinerator give the requisite temperatures (typically 1900 °F/1310 K at the burner sampling location and 1600 °F/1140 K at the exhaust) for the calculation, and volumetric flowrates at both sampling locations were determined by mass balance, after accounting for minor air leakage into the system. At the peaks of the stronger puffs, complete extinction of the laser beam occurs (on the level of the signal digitization), resulting in underestimation of the peak transient soot volume fraction.

Contributions to Puff Magnitude

The time-integrated values of soot mass are shown in Figure 8 as a function of the puff-integrated CO mass for a given puff test series. As is evident from this figure, the TDL-derived soot values show a more consistent correlation with the CO concentrations than the filter-derived soot measurement, especially at the exhaust, where the linear correlation coefficient values range from r^2 = 0.90–0.95 for the TDL-derived soot and from r^2 = 0.20–0.30 for the filter technique. Because one might expect a correlation between soot concentrations and CO levels to exist (for a given puff waste type and measurement location), determination of the soot mass on the basis of the TDL attenuation records appears quite promising.

The slope values for the linear fits in Fig. 8 show a factor of 5 difference in absolute soot levels for the two methodologies at the burner sampling location, but no discernable difference at the exhaust. The filter measurement technique tends to underestimate soot concentrations due to deposition of soot onto the inner probe walls. The deposition of soot on the walls of the sample tube is primarily due to thermophoresis, which might explain the substantial losses in soot sampling that appear to occur at the high-temperature burner sampling location. Another possible explanation is that the flow is more stratified at the burner sampling location, so the soot concentrations sampled with the probe may not be representative of the full flow cross-section at that location. The filter collection technique also suffers from an inconsistent, high detection limit,

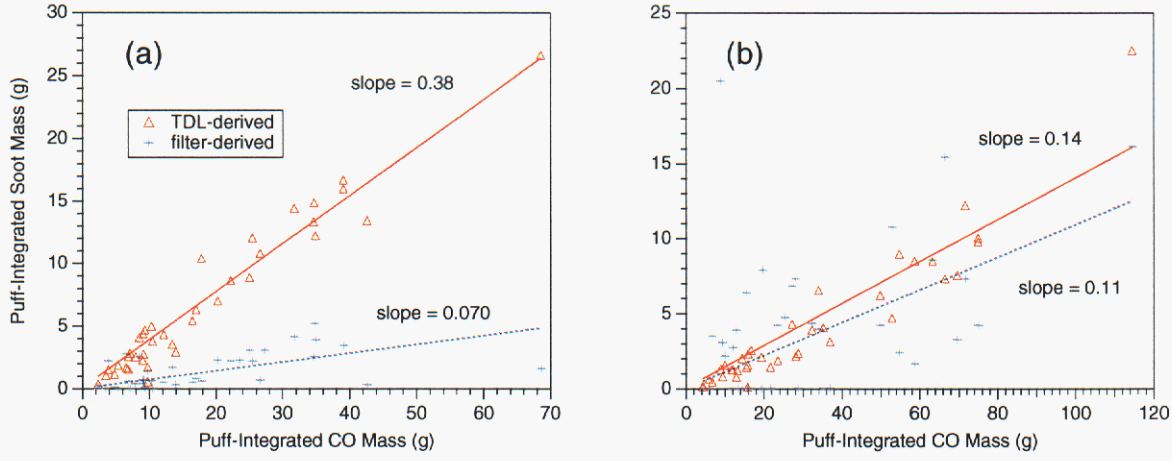

Figure 8. Puff-integrated soot mass based on both TDL attenuation and filter collection as a function of the puff-integrated CO mass: (a) burner sampling location, (b) exhaust sampling location. Puffs were generated by computer-controlled injection of methylene chloride and toluene into the kiln.

due to uncertainties associated with weighing the filter and humidity effects. This trend is evident in the large numbers of negligible filter collection weights in the exhaust sampling shown in Fig. 8b. Previous research at the EPA has shown that, although the filter technique does not quantitatively compare with established particulate measurement protocols (such as the SASS technique – source assessment sampling system), the filter trends tend to correlate well with the actual soot concentrations (Lemieux et al., 1990). The results shown in Fig. 8 confirm this for a given sampling location, but also reveal that significant differences exist in the relative errors associated with filter sampling at the burner and at the exhaust.

It appears from this analysis that the TDL-derived integrated soot mass measurements allow a more accurate determination of the composition of puffs than is possible with the filter weight soot values. Figure 9 shows the TDL values for puff-integrated soot content as a function of the total puff magnitude, together with the CEM-determined CO and THC contributions. All of these quantities are expressed in terms of the moles of molecular oxygen (O_2) required to fully oxidize the individual or total contributions of CO, hydrocarbons, and soot within the puff (Lemieux et al., 1995). These "P" values are calculated using the CEM-measured CO and THC concentrations and the TDL-derived soot mass, the volumetric flowrates in the incinerator at the positions sampled, and the stoichiometric requirement for full oxidation of the species of interest. The linear relationship of the three contributing elements to the total puff magnitude that is observed at the burner sampling location suggests that the relative contribution of these different constituents to the total puff magnitude is fairly constant over the wide range of puff intensities investigated in this work. The values of the slopes of the linear fits of the data reveal that soot dominates the unburned matter in the puffs investigated here at the burner location, accounting for 60% of the puff magnitude, with most of the remainder due to CO. By the time these puffs pass the exhaust sample port, the hydrocarbons and soot have been further oxidized and the CO dominates over the soot in contributing to the puff magnitude. In general, Figs. 7-9 show that the TDL-derived soot and the CEM-determined THC levels in the puffs are decreasing between the burner and the exhaust, whereas the CO concentrations are increasing, with no significant dependence on the overall puff magnitude. These observations suggest that the puff is slowly oxidizing (to CO)

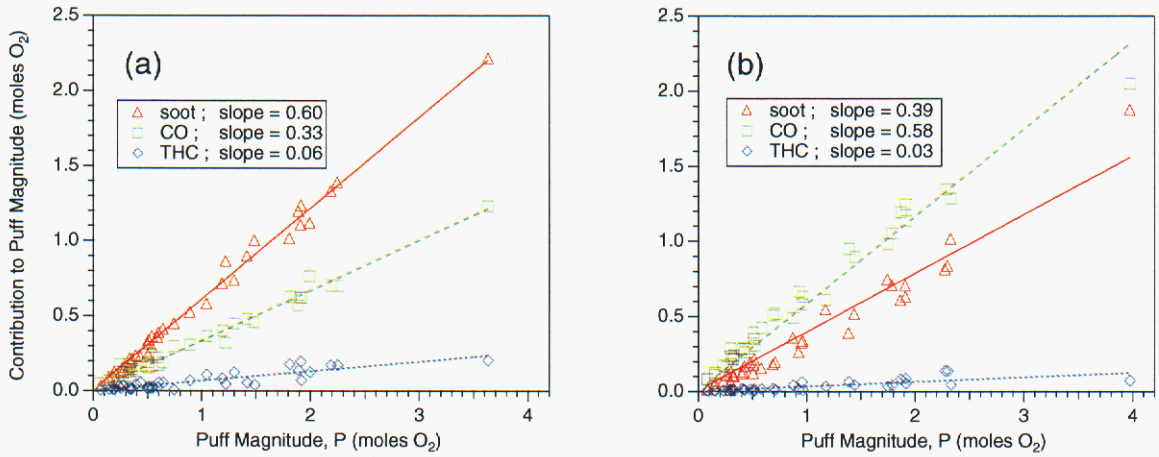

Figure 9. Time-integrated soot, CO, and THC as a function of total integrated puff magnitude for the two RKIS sample locations: (a) burner sampling location, (b) exhaust sampling location. Puffs were generated by computer-controlled injection of methylene chloride and toluene into the kiln.

during its passage through the incinerator (the afterburner was run slightly fuel lean during these experiments).

Canister Puffs

The ramrod injection of cardboard canisters containing corncob with adsorbed surrogate waste yielded puffs whose peak intensity was greater than for the liquid-lance-generated puffs used in this test series. However, the overall puff durations and integrated puff magnitudes were less than for the Phase 2 tests. These trends are evident in Figure 10, wherein a typical TDL transmittance record and the corresponding TDL gas cell (CH_4 laser) and THC CEM time traces are shown at the burner location. Attenuation of the TDL laser beams was even more severe than for the Phase 2 puffs, such that, as for Phase 2, the molecular TDL signals were not evident for the *in situ* measurements. The CH_4 TDL signals from the extractive sample gas cell show good signal-to-noise behavior and no substantial interferences. Comparison of the TDL CH_4 signal trace with the THC CEM shows qualitative agreement, though the finite filling time and flush time of the gas cell result in a peak lag and overall longer duration for the puff signal given by the extractive TDL system in comparison to the THC CEM.

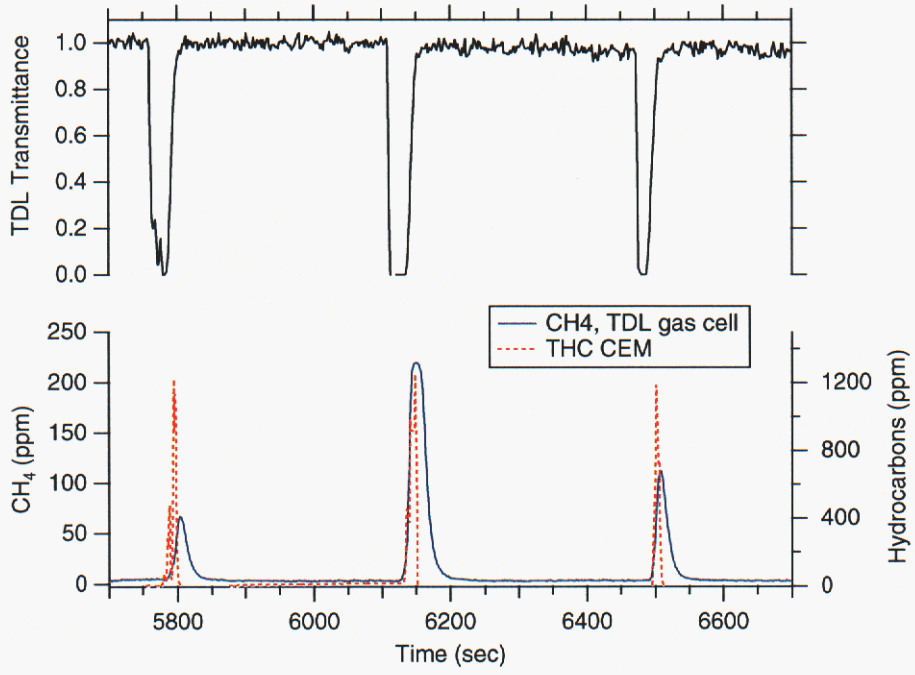

Figure 10. Time record of TDL signals and the THC CEM measurements from the RKIS burner sample location during a series of methylene chloride/toluene puffs generated by ramrod injection of corncob-containing canisters into the kiln.

Figure 11 shows the contributions of soot, CO, and hydrocarbons to the total puff magnitude for the canister puff test series. Comparison of the overall puff magnitudes at the exhaust measurement location to those at the burner reveals that considerable oxidation of the smaller puffs in this test series occurs as they traverse the transition section and secondary combustion chamber (between the two sampling locations). Also, in contrast to the results for the Phase 2 liquid-injected puffs, the CO concentrations do not follow a monotonic trend with overall puff magnitude. Rather, CO

contributions to the puff magnitude are comparable to soot for the small canister-derived puffs, but as the puff magnitude increases the CO contribution peaks and soot begins to dominate the overall composition, especially at the burner sampling location. As was found during the Phase 2 tests, the unburned hydrocarbons represent a small portion of the unburned mass of the puff.

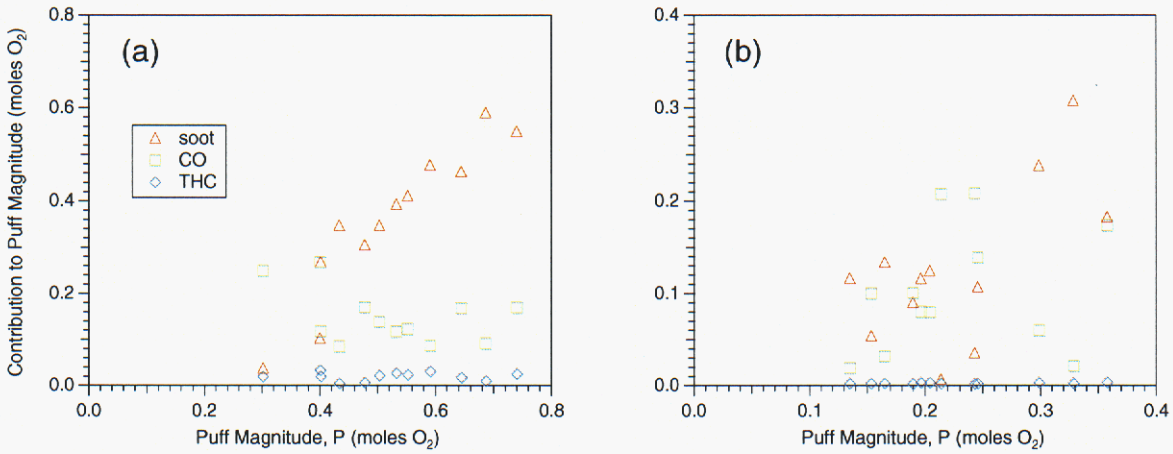

Figure 11. Time-integrated soot, CO, and THC as a function of total integrated puff magnitude for the two RKIS sample locations: (a) burner sampling location, (b) exhaust sampling location. Puffs were generated by ramrod injection of corncob-containing canisters into the kiln.

Conclusions

Steady, fuel-rich operation of the EPA's pilot-scale rotary kiln incinerator demonstrates that near-IR TDLs can be used to detect CH_4 (and possibly CO) *in situ*. For the magnitudes of the methylene chloride/toluene puffs generated in this test series, however, severe attenuation of the TDL laser beams occurs, resulting in an inability to measure *in situ* gas species concentrations during these transient events. TDL measurements of CH_4 and CO in an extractively sampled, ambient-temperature gas cell show good sensitivity and excellent agreement with corresponding solid-state gas analyzers. In addition, the *in situ* laser attenuation signals themselves can be used to calculate instantaneous soot concentrations and the total integrated soot mass contained within a puff. These continuous soot measurements provide important information for potential feed-forward operation of the kiln afterburner and also demonstrate that the quantitative accuracy of filter-based soot measurements is limited. The relative contributions of CO, soot, and total hydrocarbons to the puff composition were found to be independent of puff magnitude for puffs generated by liquid injection of the surrogate waste. For sorbent canister-derived puffs, significant oxidation of the puff occurred within the incinerator and the puff composition varied with the magnitude of the puff. The results from these experiments suggest that a combination of *in situ* and extractive gas cell TDL measurements holds the most promise for a fast-responding, quantitative puff sensor system that can accommodate upset conditions with a range of transient particle loadings.

References

Allendorf, S.W., Ottesen, D.K., Johnsen, H.A., Wang, J., Frish, M.B., Trembley, D.G., Severance, R., and Boni, A.A (1994), "Tunable diode lasers as continuous emission monitors for thermal waste treatment processes," *Proc. Int'l. Incineration Conf.*, Houston, TX, May 9-13, p. 81.

Allendorf, S.W., Ottesen, D.K., and Frish, M.B., "Tunable diode lasers: a new tool for continuous emissions monitoring and process control in thermal treatment processes," SAND95-8674, Sandia National Labs internal report, Livermore, CA, July 1995.

Allendorf, S., Ottesen, D., and Johnsen, H., "Process monitoring and control: ammonia measurements in off-gases," SAND97-8258, Sandia National Labs internal report, Livermore, CA, May 1997.

Bohren, C.F., and Huffman, D.R., Absorption and Scattering of Light by Small Particles, Wiley, New York, NY, 1983.

Cooper, D.E., and Martinelli, R.U. (1992), "Near-infrared diode lasers monitor molecular species," *Laser Focus World,* November, p. 133.

Cundy, V.A., Sterling, A.M., Lester, T.W., Jakway, A.L., Leger, C.B., Lu, C., Montestruc, A.N., and Conway, R.B. (1991), "Incineration of xylene sorbent packs: a study of conditions at the exit of a full-scale industrial incinerator," *Envir. Sci. and Tech.* **25**:223.

Dalzell, W.H., and Sarofim, A.F. (1969), "Optical constants of soot and their application to heat-flux calculations," *J. Heat Transfer* **91**:100.

Faeth, G.M., and Köylü, Ü.Ö. (1995), "Soot morphology and optical properties in nonpremixed turbulent flame environments," *Combust. Sci. and Tech.* **108**:207.

Glassman, I., *Twenty-Second Symposium (International) on Combustion*, The Combustion Institute, Pittsburgh, PA, 1988, p. 295.

Habib, Z.G., and Vervisch, P. (1988), "On the Refractive Index of Soot at Flame Temperature," *Combust. Sci. and Tech.* **59**:261–274.

Hinds, W.C., Aerosol Technology: Properties, Behavior, and Measurement of Airborne Particles, Wiley, New York, NY, 1982.

Köylü, Ü.Ö. and Faeth, G.M. (1996), "Spectral extinction coefficients of soot aggregates from turbulent diffusion flames," *J. Heat Transfer* **118**:415.

Krishnan, S.S., Lin, K.-C., and Faeth, G.M. (2000), "Optical Properties in the Visible of Overfire Soot in Large Buoyant Turbulent Diffusion Flames," *J. Heat Transfer* **122**(3):517–524.

Krishnan, S.S., Lin, K.-C., and Faeth, G.M. (2001), "Extinction and Scattering Properties of Soot Emitted from Buoyant Turbulent Diffusion Flames," *J. Heat Transfer* **123**(2):331–339.

Lee, S.C., and Tien, C.L., *Eighteenth Symposium (International) on Combustion*, The Combustion Institute, Pittsburgh, PA, 1981, p. 1159.

Lemieux, P.M., Linak, W.P., McSorley, J.A., Wendt, J.O.L., and Dunn, J.E. (1990), "Minimization of transient emissions from rotary kiln incinerators," *Combust. Sci. and Tech.* **74**:311.

Lemieux, P.M., Linak, W.P., McSorley, J.A., and Wendt, J.O.L. (1992), "Transient suppression packaging for reduced emissions from rotary kiln incinerators," *Combust. Sci. and Tech.* **85**:203.

Lemieux, P.M., Miller, C.A., Fritsky, K.J., and Chappell, P.J. (1995), "Development of an artificicial-intelligence-based system to control transient emissions from secondary combustion chambers of hazardous waste incinerators," *Proceedings: 1995 International Incineration Conference*, May 8-12, 1995, Seattle, WA.

Lemieux, P.M., Miller, C.A., Allendorf, S.W., Ottesen, D.K., Shaddix, C.R., and Touati, A. (1997), "The application of tunable diode lasers as a fast-response system to measure transient emissions from rotary kilns," *Proceedings: 1997 International Incineration Conference*, May 12-16, 1997, Oakland, CA.

Lester, T.W., Cundy, V.A., Montestruc, A.N., Leger, C.B., and Sterling, A.M. (1990), "Dynamics of rotary kiln incineration of toluene sorbent packs," *Combust. Sci. and Tech.* **74**:67.

Linak, W.P., Kilgroe, J.D., McSorley, J.A., Wendt, J.O.L., and Dunn, J.E. (1987a), "On the occurrence of transient puffs in a rotary kiln incinerator simulator: I. Prototype solid plastic wastes," *J. Air Poll. Cont. Assoc.* **37**:54.

Linak, W.P., McSorley, J.A., Wendt, J.O.L., and Dunn, J.E. (1987b), "On the occurrence of transient puffs in a rotary kiln incinerator simulator: II. Contained liquid wastes on sorbent," *J. Air Poll. Cont. Assoc.* **37**:934.

McKinnon, J.T., Abraham, E., and Miller, J.H. (1992), "An Infrared Laser Fault Detection Method for Hazardous Waste Incineration," *Combust. Sci. and Tech.* **85**:391.

Morse, J.S., and Cundy, V.A. (1994), "Sooting in chlorinated hydrocarbon combustion – a critical review," *Combust. Sci. and Tech.* **95**:333.

Mulholland, G.W., and Choi, M.Y. (1998), "Measurement of the Mass Specific Extinction Coefficient for Acetylene and Ethene Smoke Using the Large Agglomerate Optics Facility," *Proc. Comb. Instit.* Vol. 27, pp. 1515–1522.

Pershing, D.W., Lighty, J.S., Silcox, G.D., Heap, M.P., and Owens, W.D. (1993), "Solid waste incineration in rotary kilns," *Combust. Sci. and Tech.* **93**:245.

Silver, J.A. (1992), "Frequency-modulation spectroscopy for trace species detection: theory and comparison among experimental methods," *Appl. Optics* **31**:707.

Smyth, K.C., and Shaddix, C.R. (1996), "The Elusive History of m = 1.57 – 0.56i for the Refractive Index of Soot," *Comb. Flame* **107**:314–320.

Tillman, D.A. (1991), The Combustion of Solid Fuels and Wastes, Academic Press, San Diego, CA.

U.S. EPA (1993), "Operational parameters for hazardous waste combustion devices," EPA/625/R-93/008, U.S. EPA, Cincinnati, OH.

Vara-Muñoz, M.C., Young, K.J., and Swithenbank, J. (1995), "Development of a novel peak-seeker control system suitable for waste incinerators," *J. Instit. Energy*, **68**:85.

Wendt, J.O.L., and Linak, W.P. (1988), "Mechanisms governing transients from the batch incineration of liquid wastes in rotary kilns," *Combust. Sci. and Tech.* **61**:169.

Widman, J.F., Yang, J.C., Smith, T.J., Manzello, S.L., and Mulholland, G.W. (2003), "Measurement of the Optical Extinction Coefficients of Post-Flame Soot in the Infrared," *Comb. Flame* **134**:119–129.

Zhu, J., Choi, M.Y., Mulholland, G.W., and Gritzo, L.A. (2000), "Measurement of Soot Optical Properties in the Near-Infrared Spectrum," *Intl. J. Heat Mass Trans.* **43**(18):3299–3303.

Zhu, J., Choi, M.Y., Mulholland, G.W., Manzello, S.L., Gritzo, L.A., and Suo-Anttila, J. (2002), "Measurement of Visible and Near-IR Optical Properties of Soot Produced from Laminar Flames," *Proc. Comb. Instit.* **29**:2367–2374.

Distribution

3 Dr. Paul Lemieux
US EPA
NRMRL/APPCD
ERC Bldg MD-65
Research Triangle Park, NC 27711

3 Dr. C. Andy Miller
US EPA
NRMRL/APPCD
ERC Bldg MD-65
Research Triangle Park, NC 27711

1	MS 9001	M. E. John, 8000
1	MS 9005	R. C. Wayne, 2800
1	MS 9004	J. Vitko, 8100
1	MS 9054	W. J. McLean, 8300
1	MS 9007	D. R. Henson 8400
1	MS 9002	P. N. Smith, 8500
1	MS 9003	K. E. Washington, 8900
1	MS 9003	D. L. Crawford, 9900
3	MS 9052	C. R. Shaddix, 8361
1	MS 9052	S. W. Allendorf, 8353
1	MS 9052	L. G. Blevins, 8361
3	MS 9018	Central Technical Files, 8945-1
1	MS 0899	Technical Library, 9616
1	MS 9021	Classification Office, 8511/Technical Library, MS 0899, 9616 DOE/OSTI via URL

This page intentionally left blank